Ionics (2011) 17:811–819
DOI 10.1007/s11581-011-0585-8

ORIGINAL PAPER

Dielectric spectroscopy and confirmation of ion conduction mechanism in direct melt compounded hot-press polymer nanocomposite electrolytes

Shobhna Choudhary · R. J. Sengwa

Received: 20 October 2010 / Revised: 13 April 2011 / Accepted: 22 May 2011 / Published online: 9 June 2011

Abstract Solid-type polymer nanocomposite electrolyte (PNCE) comprising poly(ethylene oxide) (PEO), lithium perchlorate ($LiClO_4$) and montmorillonite (MMT) nano-platelets were synthesized by direct melt compounded hot-press technique at 70 °C under 3 tons of pressure. The spectra of complex dielectric function, electric modulus and alternating current (ac) electrical conductivity, and complex impedance plane plots of these materials were investigated in the frequency range 20 Hz to 1 MHz at ambient temperature. The variation of electrode polarization and ionic conduction relaxation times with MMT concentration up to 20 wt.% confirms their strong correlation with direct current ionic conductivity. The predominance of exfoliated MMT structures in PEO matrix and their effect on cation conduction mechanism and ion pairing were discussed by considering a supramolecular transient cross-linked structure. The normalized ac conductivity as a function of scaled frequency of these PNCE materials obey the universal time–concentration superposition behaviour alike the disordered solid ionic conductors.

Keywords Polymer nanocomposite electrolyte · Ionic conductivity · Dielectric relaxation · Poly(ethylene oxide) · MMT clay · Lithium perchlorate

S. Choudhary · R. J. Sengwa (✉)
Dielectric Research Laboratory, Department of Physics,
JNV University,
Jodhpur 342 005, India
e-mail: rjsengwa@rediffmail.com

Introduction

During the last decade, synthesization of poly(ethylene oxide) (PEO) and alkaline metal salt-based solid-type polymer nanocomposite electrolyte (PNCE) of improved mechanical, thermal and electrochemical stability with enhanced ionic conductivity has received extensive attention as candidate material for electrochromic devices [1–15]. The PEO-based electrolytes complexed with lithium salt and montmorillonite (MMT) nano-clay as filler have raised curiosity for research and development of solid-type novel PNCE materials for lithium batteries [1–5]. Various spectroscopic studies have justified that the exfoliated/intercalated MMT structures in polymer matrix make the polymer amorphous in terms of improving its mechanical strength, thermal stability, gas barrier, fire retardance, corrosion resistance, and also ionic conductivity [2, 5, 10, 16–22]. Further, it is revealed that the exfoliated nano-platelets of MMT in the PNCE films minimize the ion-pairing effect, whereas the intercalated MMT structures impede the polymer crystallization and enhance the nano-metric channels for cations mobility [4, 5, 7, 15, 23]. It is established that the ionic conductivity of the PNCE materials is strongly governed by the route of preparation, concentration of MMT in polymer matrix, type of alkaline metal salt used and its concentration, besides the amount of plasticizer added.

The synthesis of PNCE films using the composition of PEO, alkaline metal salt and MMT by solution–cast technique and their ions conduction characterization by dielectric/impedance spectroscopic measurements exhibit discerning investigations [1–8, 15]. As compared to the solution–cast technique, the preparation of PNCE materials by melt compounded technique is more suitable for their large-scale technological applications, owing to its rapid,

least expensive and dry procedure to prepare solvent free polymer electrolyte films [2, 10, 11, 24]. The survey reveals that so far, the PNCE films of PEO–$LiClO_4$–MMT composite have not been synthesized by direct melt compounded hot-press technique for the ion conduction characterization. The PEO is a low melting temperature hydrophilic polymer, which acts as a solid solvent in its melt state for alkaline metal salts and has the ability of direct intercalation in MMT galleries because of their hydrophilic behaviour.

In search of novel PNCE materials, this paper presents the detailed dielectric/impedance dispersion properties and relaxation processes including their correlation with the ion conduction mechanism in PEO–$LiClO_4$–MMT films prepared by direct melt compounded hot-press technique. A supramolecular transient cross-linked model of PEO/Li^+/MMT on a nanometre scale was illustrated by considering the comparative variation in their dielectric properties with the change in concentration of MMT as nano-filler.

Materials and methods

Materials

The PEO of molecular weight 600,000 g/mol, $LiClO_4$ (battery grade, dry, 99.99% metal basis) and polymer grade hydrophilic MMT clay (Nanoclay, PGV, a product of Nanocor®) were purchased from Sigma-Aldrich, USA. According to the technical data sheet of Nanocor®, the white colour MMT nano-clay platelets have thickness of only 1 nm and individual platelets have aspect ratio (length/width) from 150–200 that have 145 meq/100g cation exchange capacity (CEC), 2.6 g/cc specific gravity and 9−10 pH value (5% dispersion).

Preparation of PNCE films

For the preparation of PNCE films, firstly, PEO (2.68 g) and $LiClO_4$ (0.32 g) were taken for the 20:1 molar ratio of EO/Li^+ for each sample. After that, respective amounts of MMT—0.00, 0.0268, 0.0536, 0.0804, 0.134, 0.268 and 0.536 g with respect to the weight of PEO for the 0, 1, 2, 3, 5, 10 and 20 wt.% (*w*/*w*) MMT concentration—were taken and mechanically mixed with PEO and $LiClO_4$ for each sample using an agate mortar and pestle. The direct melt compounding of each composition was performed at 70± 1 °C, which is slightly higher than the PEO melting temperature (65 °C). The films were synthesized in 60-mm-diameter stainless steel die with 1-mm spacer using hot polymer press film making unit under 3 tons of pressure which results into melt compounded PNCE films of 1 mm in thickness. The resulting free standing solid-type PNCE films have the general formula $(PEO)_{20}-LiClO_4-x$wt.% MMT, where MMT concentration x varies from 0 to 20 wt. % with respect to the PEO weight.

Measurements

Agilent 4284A precision LCR metre and Agilent 16451B solid dielectric test fixture, having four terminals nickel-plated cobal (an alloy of 17% cobalt+29% nickel+54% iron) electrodes of 38 mm in diameter, were used for the dielectric measurements in the alternating current (ac) field frequency ranges from 20 Hz to 1 MHz. Frequency-dependent values of parallel capacitance C_p, parallel resistance R_p and loss tangent tanδ (dissipation factor, D) of the PNCE films were measured for the determination of their dielectric/electrical spectra at ambient temperature (~27±1 °C). Prior to the sample measurement, the open circuit calibration of the cell was performed to eliminate the effect of stray capacitance of the cell leads. The details of the evaluation of intensive quantities, namely complex dielectric function $\varepsilon^*(\omega) = \varepsilon' - j\varepsilon''$, complex ac electrical conductivity $\sigma^*(\omega) = \sigma' + j\sigma''$, and complex electric modulus $M^*(\omega) = M' + jM''$ and extensive quantity, i.e. complex impedance $Z^*(\omega) = Z' - jZ''$ of the films, are described by us elsewhere [11, 22, 25, 26].

Results and discussion

Complex dielectric spectra and MMT structures

Figure 1 shows the frequency-dependent real part (permittivity) ε' and imaginary part (dielectric loss) ε'' values of $(PEO)_{20}-LiClO_4-x$wt.% MMT films, which decrease non-linearly with the increase of frequency from 20 Hz to 1 MHz at 27 °C. The gradual decrease in ε' values at high frequencies (inset of Fig. 1) shows the relaxation processes corresponding to the PEO molecular polarization and the Maxwell–Wagner (MW) interfacial or ionic conduction polarization. The large increase in ε' values with decrease in the frequency below 10^4 Hz represents the significant contribution of electrode polarization (EP) process to the low-frequency dielectric dispersion in these materials.

Dielectric studies of the polymer clay nanocomposite establish the fact that the comparative changes in ε' values with the MMT concentration in the polymer matrix possess strong correlation with the intercalated/exfoliated MMT structures [17–22, 25–29]. In the PEO matrix, MMT nano-platelets form the hybrid structures (intercalated and exfoliated) due to their hydrophilic behaviour. The predominance of intercalated or exfoliated structures of MMT, respectively, governs the increase or decrease of ε' values, as compared to that of the pristine polymer matrix [22, 25–

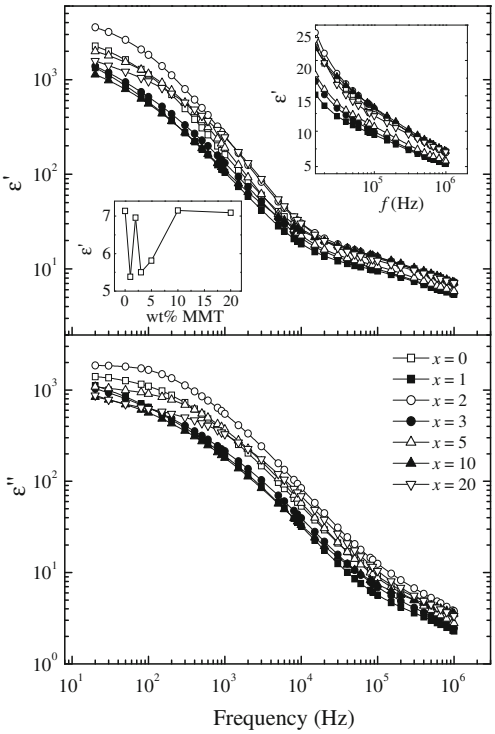

Fig. 1 Frequency-dependent real part ε' and loss ε'' of the complex dielectric function of the $(PEO)_{20}-LiClO_4-x$wt.% MMT nanocomposite electrolytes synthesized by direct melt compounded technique. *Insets* show the enlarged view at high frequencies and also the variation of ε' at 1 MHz with weight percent MMT concentration

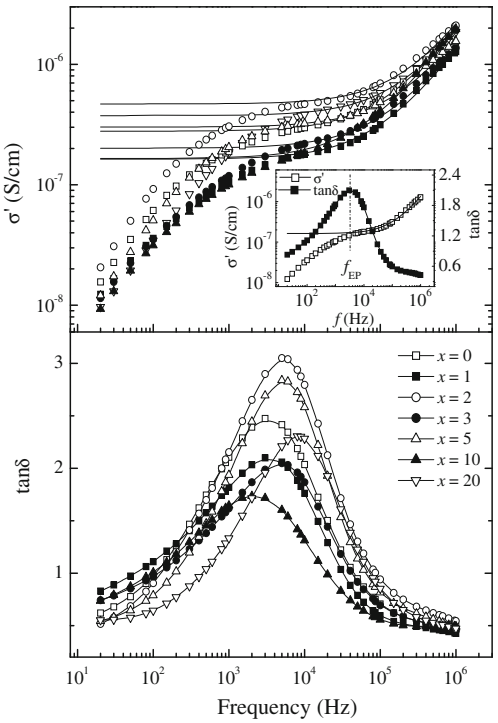

Fig. 2 Frequency-dependent real part of ac conductivity σ' and loss tangent (tanδ) of the $(PEO)_{20}-LiClO_4-x$ wt.% MMT nanocomposite electrolytes synthesized by direct melt compounded technique. The continuous solid line in σ' spectra represents the fit of experimental data using the Origin® non-linear curve fitting software to the Jonscher power law $\sigma'(\omega) = \sigma_{dc} + A\omega^n$. *Inset* shows the correlation in f_{EP} value of σ' and tanδ spectra for the 1 wt.% MMT PNCE film

29]. The inset of Fig. 1 shows that the ε' values at 1 MHz of the studied PNCE films anomalously vary with the increase of MMT concentration, and these values are comparatively smaller or equal than that of the PNCE film without MMT. The comparative ε' values at 1 MHz frequency reveal the predominance of MMT exfoliated structures at 1, 3 and 5 wt.%, whereas at 2, 10 and 20 wt.%, there is the formation of equal amounts of exfoliated and intercalated MMT structures in these melt compounded PNCE films.

ac conductivity spectra

Figure 2 exhibits frequency-dependent values of the real part of ac conductivity, σ', of the melt compounded $(PEO)_{20}-LiClO_4-x$wt.% MMT films of varying MMT concentration. These spectra have a direct current (dc) conductivity plateau in the middle frequency region and exhibit conductivity dispersions in the lower- and higher-frequency regions. The σ' values of the PNCE films were fitted using the Origin® non-linear curve fitting software to the Jonscher power law [30]:

$$\sigma'(\omega) = \sigma_{dc} + A\omega^n \quad (1)$$

where σ_{dc} is the dc ionic conductivity, A is the pre-exponential factor and n is the fractional exponent ranging between 0 and 1 for the ion conducting electrolytes. The solid line in the σ' spectra (Fig. 2) denotes the fit of experimental data to the power law expression (Eq. 1), and the obtained fit values of σ_{dc}, A and n are recorded in Table 1. The exact overlapping of the fit line and experimental points of the σ' values of the investigated PNCE materials in the high-frequency region confirms their power law behaviour. The deviation from σ_{dc} (plateau region) value in lower-frequency region of the σ' spectra is due to the contribution of EP process, which can be analyzed for the estimation of mobile ion concentration and their mobility in the polymer electrolytes [31–33]. The n values of the investigated PNCE films were found in the range 0.87 to 0.91, and their σ_{dc} values vary anomalously with the increase of MMT concentration (Table 1).

The loss tangent (tan$\delta=\varepsilon''/\varepsilon'$) spectra of the investigated PNCE films of different MMT concentrations are plotted in Fig. 2. These spectra have peaks in the frequency range 10^3 to 10^4 Hz, which correspond to the electrode polarization relaxation frequency, f_{EP} [11, 18–21, 31]. The f_{EP} separates the bulk material properties from the contribution of EP process, which occurs in the lower-frequency region due to formation of electric double layers (EDLs) (also known as blocking layers) by the free charges that build up at

Table 1 Jonscher power law $\sigma'(\omega) = \sigma_{dc} + A\omega^n$ fit values of dc ionic conductivity σ_{dc}, pre-exponent factor A, and fractional exponent n and most probable ionic conductivity relaxation time τ_σ and electrode polarization relaxation time τ_{EP} with varying MMT concentration ($x$wt.%) of the $(PEO)_{20}-LiClO_4-x$wt.% MMT nanocomposite electrolytes

MMT ($x$wt.%)	$\sigma_{dc}\times10^7$ (S cm^{-1})	$A\times10^{12}$	n	τ_σ (μs)	τ_{EP} (μs)
0	2.78	1.46	0.89	3.53	50.49
1	1.63	1.30	0.88	4.95	49.23
2	4.69	1.17	0.91	1.83	29.58
3	2.01	1.53	0.87	3.73	30.71
5	3.01	1.24	0.89	2.46	29.58
10	1.65	1.67	0.89	8.25	77.94
20	3.75	1.27	0.90	2.19	19.04

interface between the dielectric material and the metallic electrode surfaces in plane geometry [18, 31]. Inset of Fig. 2, which displays the σ' and tanδ values for 1 wt.% MMT concentration PNCE film as representative plot, shows that the value of f_{EP} corresponds to the tanδ peak and the frequency value at which the lower-frequency σ' spectra deviate from the σ_{dc} plateau are the same. This observation confirms the suitability of both tanδ and σ' spectra of PNCE materials for the characterization and analysis of the EP phenomena affected frequency region. The electrode polarization relaxation time τ_{EP}, which involves charging and discharging time of the EDLs capacitances, is determined by the relation $\tau_{EP} = (2\pi f_{EP})^{-1}$ [11, 34]. The evaluated τ_{EP} values of the PNCE films are recorded in Table 1 which vary anomalously with the increase of MMT concentration.

ac conductivity universality master curves

Dyre et al. [35, 36] in review articles attempted various macroscopic and microscopic models in glasses, polymers, nanocomposites and other disordered solids to explain the physics of dc and ac ions conduction, wherein it is found that the scaling function associated with the random barrier model (hopping conduction) is universal, which means that the shape of master curves of normalized ac conductivity as a function of scaled frequency for all the ion-conducting disordered materials at varying composition and temperature obeys time–temperature–concentration superposition.

The scaling behaviour of ac conductivity $\sigma'(\omega)/\sigma_{dc}$, which is also known as normalized ac conductivity can be described by Jonscher power law Eq. 1 with the following relation:

$$\sigma'(\omega)/\sigma_{dc} = 1 + (\omega/\omega_0)^n \quad (2)$$

where $\omega_0=(\sigma_{dc}/A)^{1/n}$ is a characteristic ionic conduction relaxation frequency ($\omega_0 = \omega_\sigma = 2\pi f_\sigma$), which is used as scaling parameter for frequency axis. This scaling relation predicts that $\sigma'(\omega)$ starts to rise when the applied frequency is greater than ω_0. Figure 3 shows the scaling behaviour of $\log(\sigma'/\sigma_{dc})$ versus $\log(\omega/\omega_0)$ of the investigated PNCE films of varying MMT concentration. For these electrolytes, it is found that the scaled ac conductivity spectra collapse on a single common curve in the upper frequency region, which suggests that the ion conduction can be demonstrated by the random barrier model (RBM) (symmetric hopping model) [35]. The deviation from scaled spectra at low frequencies is due to the contribution of electrode polarization (EP) effect [37]. The upper layer in Fig. 3 shows the EP effect corrected normalized ac conductivity $\log(\sigma'_{corr}/\sigma_{dc})$ versus scaled frequency $\log(\omega/\omega_0)$ plots. It is found that all the curves of normalized ac conductivity collapse on a single master curve over the entire scaled frequency for these PNCE materials. Results confirm that similar to ion-conducting glasses, melt compounded PNCE materials also obey the ac conductivity universality. Further, the n values of these materials which range from 0.87 to 0.91 (Table 1) also favours the RBM type ion conduction mechanism of disordered solid ion conductors [35–37].

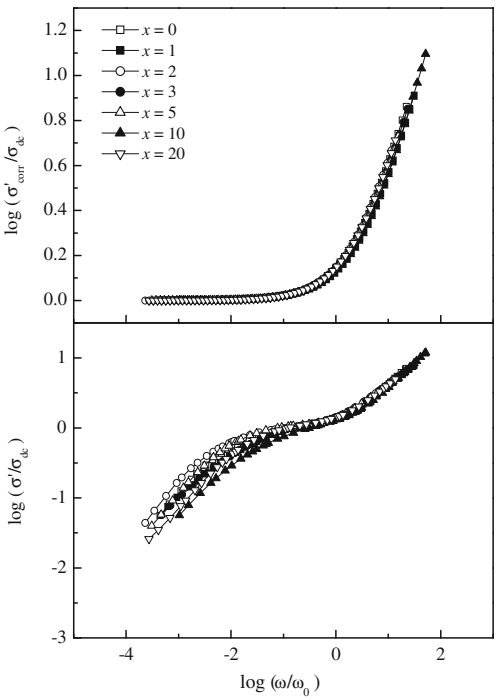

Fig. 3 Log–log plots of normalized ac conductivity, $\log(\sigma'/\sigma_{dc})$ and electrode polarization contribution subtracted normalized ac conductivity, $\log(\sigma'_{corr}/\sigma_{dc})$ versus scaled frequency $\log(\omega/\omega_0)$

Electric modulus spectra

Figure 4 shows that the real part of electric modulus M' of the investigated PNCE films increases non-linearly with the increase of frequency, whereas ionic conductivity relaxation peaks were observed in the spectra of loss part of electric modulus M'' in the higher-frequency region. Similar shape of M'' spectra was also reported for the solution–cast PEO-based PNCE films of varying MMT concentrations [6, 7]. The value of ac conductivity relaxation frequency f_σ of the cation coordinated PEO segmental motion, which contributed to the MW interfacial polarization, was determined from the intersection of M' and M'' spectra shown in the inset of Fig. 4 for 1 wt.% MMT concentration PNCE film as representative plot. The MW process occurs owing to the free charges build up during the short-range electromigration at the interfacing boundaries of various components of different dielectric constant (or conductivities) in the composite material, which results in the formation of nanocapacitors in the electrolyte material. At sufficient high frequencies, such short-range movements of free charges cannot follow the fast changes developed in the applied ac field; only the molecular polarization is contributed to the dielectric dispersion process. The f_σ separates the change in ions from dc to ac transport, value of which is used for the evaluation of the most probable ionic conduction relaxation time τ_σ using the relation $\tau_\sigma = (2\pi f_\sigma)^{-1}$ [11, 34]. The τ_σ values, thus evaluated, of the investigated PNCE films are recorded in Table 1.

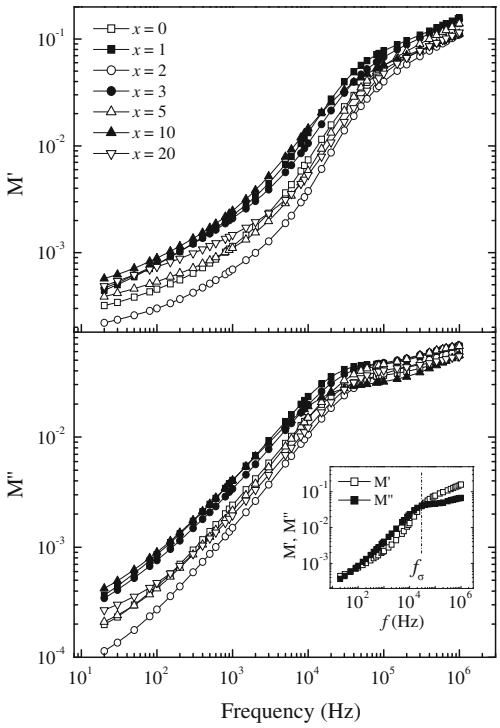

Fig. 4 Frequency-dependent real part M' and loss M'' of complex electric modulus of the $(PEO)_{20}-LiClO_4-x$ wt% MMT nanocomposite electrolytes synthesized by direct melt compounded technique. *Insets* show the intersection of M' and M'' spectra at f_σ for the 1 wt.% MMT PNCE film

Impedance behaviour

Figure 5 shows the complex impedance plane plots (Z'' versus Z') for the studied PNCE films, and inset shows the enlarged view of the plots at high frequencies. The frequency values of the data points in these plots increase, going from right to left on the arcs. These plots have semicircular arcs in high-frequency region corresponding to bulk material properties and are followed by a spike in the lower-frequency region, which corresponds to formation of EDL capacitances at the electrode/electrolyte interface. The intercept on real axis Z' of the common part of two arcs gives the value of dc resistance, R_{dc}, of the bulk material as marked in the inset of Fig. 5 for the 2 wt. % MMT concentration PNCE film. The thickness of film t_g, effective surface area of cell electrode S, and R_{dc} are commonly used for the evaluation of σ_{dc} value by the relation $\sigma_{dc} = t_g/SR_{dc}$[15, 38]. We have determined the exact values of σ_{dc} by power law fit to the σ' spectra (Fig. 2). From inset of Fig. 5, it can be seen that the R_{dc} values of these PNCE materials vary anomalously in the range tens of kilo-ohm with the increase of MMT concentration.

Dielectric relaxation times and ionic conductivity correlation

Generally, for electrolytes, ionic conductivity is defined by the relation $\sigma_{dc} = \Sigma n_i \mu_i q_i$, where n_i, μ_i and q_i refer to the charge carriers density, the ions mobility and the charge of

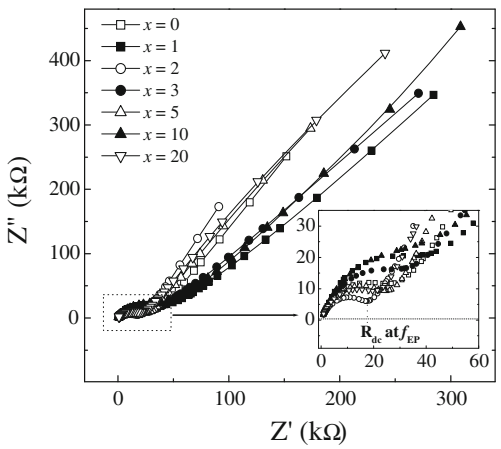

Fig. 5 Z'' versus Z' plots of the $(PEO)_{20}-LiClO_4-x$wt.% MMT nanocomposite electrolytes synthesized by direct melt compounded technique. *Inset* shows enlarged view of the plots in higher-frequency region

*i*th ion, respectively [7, 11]. In polymer/alkaline metal salt/MMT nanocomposite electrolytes, the barrier produced by the dispersed MMT nano-platelets between anions and the polymer coordinated cations reduces the ion-pairing effect, which influences their ionic conductivity at fixed concentration of the salt. Further, the enhancement in amorphous phase of the intercalated polymer in MMT galleries and its segmental dynamics increases the ionic conductivity of the PNCE materials.

In PEO–MMT nanocomposites, the intercalated MMT platelets impede the PEO crystallization and form some kind of tunnel (nanometric channels) that increases the cations mobility coordinated with PEO chain in the MMT galleries [39–41]. At ambient temperature, the σ_{dc} of pure PEO is nearly 10^{-10} S cm^{-1} [11, 42], which increases sharply to 2.78×10^{-7} S cm^{-1} with the addition of $LiClO_4$ at the molar ratio 20:1 of the PEO monomer unit EO to the Li^+ in the PEO–$LiClO_4$ composite (Table 1). The increase in ionic conductivity by three orders of magnitude at ambient temperature with 20:1 concentration of EO/Li^+ in PEO–$LiClO_4$ electrolyte reveals the large dissociation of the salt ions in melted PEO solvent during melt compounding process. The ionic conductivity values of direct melt compounded PEO–$LiClO_4$ film at ambient temperature were found in good agreement to that of the PNCE film prepared by solution–cast technique [1, 2, 5, 12–14].

Figure 6 shows that the σ_{dc} values of $(PEO)_{20}-LiClO_4-x$wt.% MMT films vary anomalously in the range ~1.5×10^{-7} to 5×10^{-7} S cm^{-1} (Table 1) with the increase of MMT concentration. At 2 wt.% MMT, the σ_{dc} value of the PNCE film is nearly two times that of the MMT free electrolyte film. Regarding the dynamics of polymer on one hand, a close contact of polymer segments to a rigid inorganic (MMT) structure may slow down their local chain motion. On the other hand, dimensional restrictions in the nanometer range may have an effect on the cooperativity of motional process possibly leading to enhanced polymer mobility. The anomalous variation in dielectric relaxation times (τ_{EP} and τ_{σ}) with the increase of MMT concentration of the studied PNCE films reveals that the PEO interactions in complex composite and the predominance amount of intercalated/exfoliated MMT in PEO matrix vary with the MMT concentration. A good resemblance of the σ_{dc} values with the variation in τ_{EP} and τ_{σ} values up to 20 wt.% MMT concentration (Fig. 6) confirms that the ionic conductivity and dielectric relaxation processes in these PNCE materials have strong correlation, i.e. the σ_{dc} value increases due to the increase of cation mobility as evidenced by decrease of τ_{EP} and τ_{σ} values and vice versa. Similar correlation behaviour of conductivity versus relaxation time is also observed in the melt compounded PNCE films of sodium salts [11]. Further, it is observed that the σ_{dc} values obey the variation of ε' values at 1 MHz up to 5 wt.% MMT loading

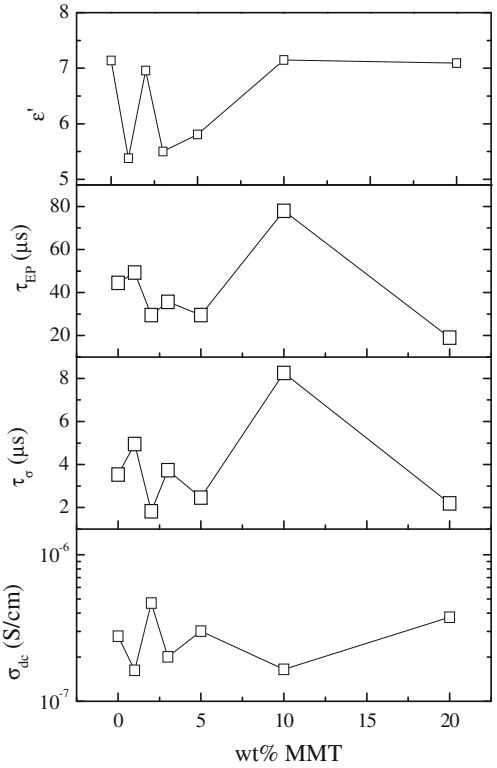

Fig. 6 MMT clay concentration dependent ε' values at 1 MHz, electrode polarization relaxation time τ_{EP}, ionic conduction relaxation time τ_{σ} and dc ionic conductivity σ_{dc} of the $(PEO)_{20}-LiClO_4-x$wt.% MMT nanocomposite electrolytes synthesized by direct melt compounded technique. For clarity, *error bars* are not indicated. *Error bars* are smaller than the size of the *symbols*

(Fig. 6). Recently, Furlani et al. [43] confirmed the strong correlation between the dielectric relaxation times, relaxation strength and ionic conductivity in lithium-doped PEO of average molecular weight 400 g/mol based electrolytes at ambient temperature. The small amount of MMT in PEO matrix significantly increases the mechanical and thermal strength of the PEO–MMT nanocomposite materials [10, 16]. Considering this fact, along with the observed σ_{dc} values, it can be suggested that the PNCE film of $(PEO)_{20}-LiClO_4-2$ wt.% MMT prepared by direct melt compounded technique at PEO melting temperature can serve comparatively more suitable solid-type ion conductor of improved mechanical and thermal strength.

PNCE transient structures

In general, a number of models have been proposed by considering the Lewis acid–base type polymer/cation/MMT interactions using different spectroscopic results to explain the ion conduction mechanism in PNCE materials [2, 3, 10]. Here, we propose a model (Fig. 7) on the basis of dielectric parameters of the investigated PNCE materials to

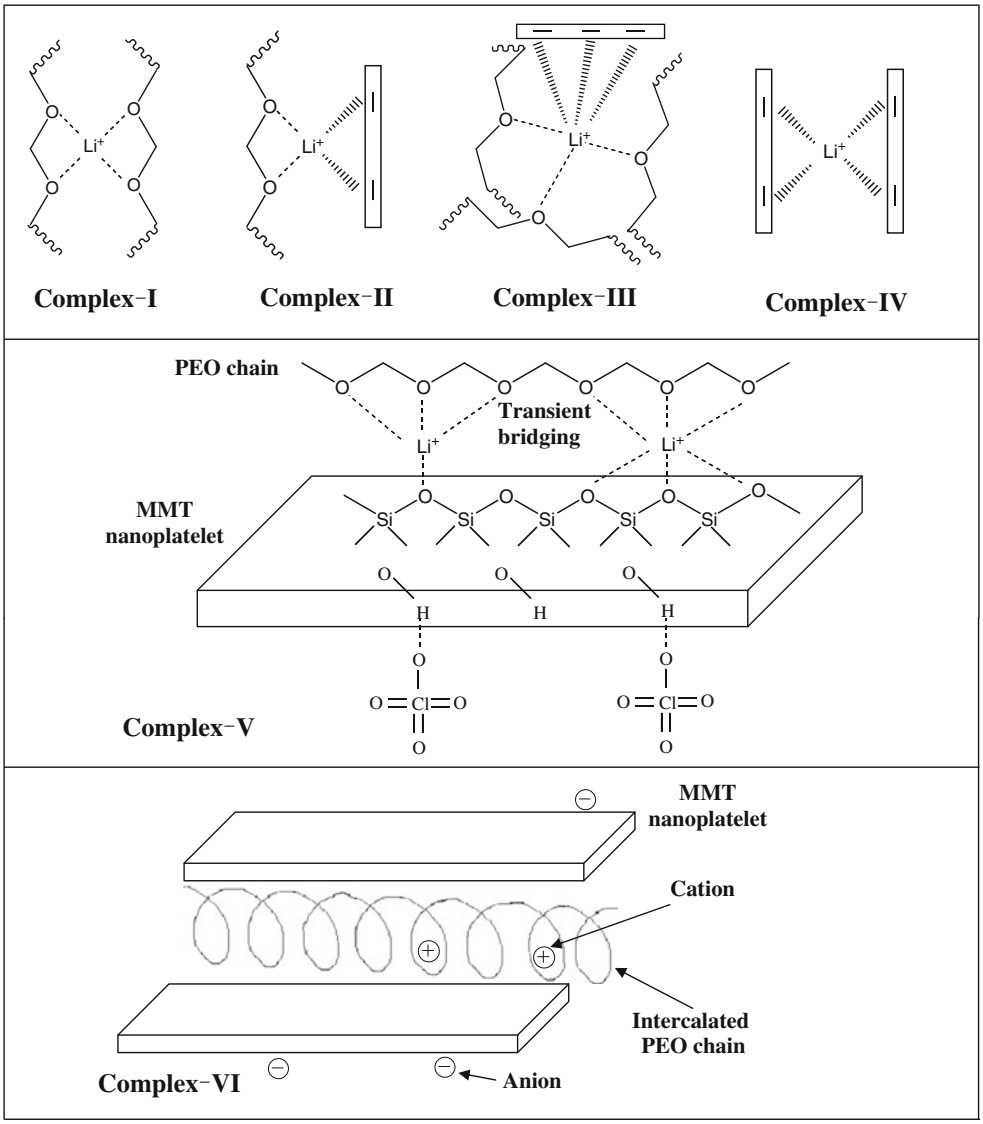

Fig. 7 Schematic illustration of PEO–Li^+–MMT interactions: PEO complex with Li^+ (*complex I*), PEO and MMT complexes with Li^+ (*complex II and III*), MMT complex with Li^+ (*complex IV*), transient cross-linking of PEO and exfoliated MMT nano-platelet through Li^+ (*complex V*), Li^+ coordinated PEO intercalation in MMT gallery (*complex VI*)

explain the effect of various interactions on the PEO local chain dynamics and the mechanism of PEO coordinated lithium cation motion.

It is generally agreed that the Li^+ ion has four to six sites of coordination with PEO and MMT nano-platelets [2, 10]. In Fig. 7 (complex I), the Li^+ coordination with four neighbour etheric oxygens of the PEO segments in PEO–Li^+ domain is depicted. Similarly, in the PEO–Li^+–MMT domain, the exfoliated MMT and etheric oxygen of PEO can form the complexes with Li^+ as depicted in complex II and complex III, but within the MMT domain, Li^+ can coordinate with the MMT siloxane groups as depicted in complex IV of Fig. 7.

The formation of possible supramolecular transient cross-linked structure between PEO and exfoliated MMT nano-platelet is sketched in complex V, whereas the cation coordinated PEO intercalation in MMT gallery is sketched in complex VI of Fig. 7. The strength of bridging (potential barrier) between PEO/Li^+/exfoliated MMT interactions governs the PEO segmental dynamics and also the collective translational motion of the Li^+ ions coupled to PEO motion as per the concept of random barrier model for cation motion [35–37]. The effective potential barrier for the Li^+ cation mobility in the dynamical complex structure of nanocomposite results in the variation of ionic conductivity with the change in MMT concentration.

Generally, the anions (ClO_4^-) exist somewhere in the polymer backbone as an un-coordinated in the electrolyte films of without MMT. Due to bulkiness, these anions are almost immobile and rarely contributed in the ionic conduction. In MMT-filled PNCE, there is a large probability of the existence of bulky anions outside the MMT galleries, but the PEO coordinated cations have natural tendency to enter into MMT nanometric galleries (intercalated structure) during their synthesis by melt compounding under pressure (complex VI of Fig.7). Due to the formation

of such complexes, the ion pairing is prevented, and the ionic conductivity is due to the cation mobility coupled to the PEO segmental motion. But exfoliated MMT structures and their interactions produce some hindrance to cation motion and also reduce the nanometric cations conduction paths. The synthesization of the PNCE by direct melt compounded technique under pressure has a large tendency of the orientation of intercalated/exfoliated MMT nano-platelets parallel to the film surface, which affected the ion conduction paths, and hence, such oriented structures may also contribute to the ionic conductivity. Due to high aspect ratio of MMT nano-platelets, they are able to maintain parallelism after intercalation of PEO chain under pressure. Therefore, the cation mobility in the investigated PNCE films depends not only on the PEO segmental motion and the available ion conduction paths but also on the height of potential barrier that the cation must overcome to move from one site to another in the complex network. The supramolecular complex model illustrated in Fig. 7 is suitable to explain the mechanism of Li^+ cation conduction coupled with PEO chain dynamics in the $(PEO)_{20}-LiClO_4-x$wt.% MMT nanocomposites.

Conclusions

This article reports the dielectric spectroscopy and various dielectric relaxation processes, and their correlation with the cation conduction mechanism in $(PEO)_{20}-LiClO_4-x$wt.% MMT nanocomposite films prepared by direct melt compounded hot-press technique. On the basis of the structural information extracted from the comparative values of various dielectric parameters, the supramolecular transient structure of the complexations of studied PNCE films was proposed. The anomalous behaviour of the ionic conductivity of these PNCE materials with the variation of MMT concentration was explained by using the random barrier model of the disordered solid ionic conductors. The comparative analysis of various dielectric formalisms spectra and dielectric parameters associated to them provides the direct information on the hindrance to the coupled motion of cations and PEO segments in presence of dispersed exfoliated/intercalated MMT nano-platelets structures in the PEO matrix. These results establish the suitability of dielectric relaxation spectroscopy as a novel tool for the melt compounded online processing and monitoring, and off-line measurements of the PNCE materials.

Acknowledgements The authors are grateful to the DST, New Delhi for providing the experimental facilities through project No. SR/S2/CMP-09/2002. One of the authors, SC, is thankful to the UGC, New Delhi for the award of RFSMS fellowship.

References

1. Fan L, Nan CW, Dang Z (2002) Electrochim Acta 47:3541–3544
2. Chen HW, Chang FC (2001) Polymer 42:9763–9769
3. Chen HW, Chiu CY, Wu HD, Shen IW, Chang FC (2002) Polymer 43:5011–5016
4. Kim S, Hwang EJ, Jung Y, Han M, Park SJ (2008) Colloids Surf A Physicochem Eng Aspects 313–314:216–219
5. Mohapatra SR, Thakur AK, Choudhary RNP (2009) J Power Sources 191:601–613
6. Pradhan DK, Choudhary RNP, Samantaray BK (2009) Mater Chem Phys 115:557–561
7. Pradhan DK, Choudhary RNP, Samantaray BK (2008) Express Polym Lett 2:630–638
8. Pradhan DK, Choudhary RNP, Samantaray BK, Thakur AK, Katiyar RS (2009) Ionics 15:345–352
9. Pradhan DK, Samantaray BK, Choudhary RNP, Thakur AK (2005) J Power Sources 139:384–393
10. Loyens W, Maurer FHJ, Jannasch P (2005) Polymer 46:7334–7345
11. Sengwa RJ, Sankhla S, Choudhary S (2010) Ionics 16:697–707
12. Hu L, Tang Z, Zhang Z (2007) J Power Sources 166:226–232
13. Xi J, Qiu X, Cui M, Tang X, Zhu W, Chen L (2006) J Power Sources 156:581–588
14. Wang L, Yang W, Wang J, Evans DG (2009) Solid State Ionics 180:392–397
15. Thakur AK, Pradhan DK, Samantaray BK, Choudhary RNP (2006) J Power Sources 159:272–276
16. Strawhecker KE, Manias E (2003) Chem Mater 15:844–849
17. Kanapitsas A, Pissis P, Kotsilkova R (2002) J Non-Cryst Solids 305:204–211
18. Sengwa RJ, Sankhla S, Choudhary S (2009) Colloid Polym Sci 287:1013–1024
19. Sengwa RJ, Choudhary S, Sankhla S (2008) Express Polym Lett 2:800–809
20. Sengwa RJ, Choudhary S, Sankhla S (2009) Colloids Surf A Physicochem Eng Aspects 336:79–87
21. Sengwa RJ, Choudhary S, Sankhla S (2009) Polym Int 58:781–789
22. Sengwa RJ, Sankhla S, Choudhary S (2010) Indian J Pure Appl Phys 48:196–204
23. Chen-Yang YW, Chen YT, Chen HC, Lin WT, Tsai CH (2009) Polymer 50:2856–2862
24. Pandey GP, Hashmi SA, Agrawal RC (2008) Solid State Ion 179:543–549
25. Sengwa RJ, Choudhary S, Sankhla S (2010) Comp Sci Technol 70:1621–1627
26. Sengwa RJ, Choudhary S (2010) J Macromol Sci Part B Phys doi:10.1080/00222348.2010.507451
27. Sengwa RJ, Choudhary S (2010) Express Polym Lett 4:559–569
28. Wang HW, Chang KC, Yeh JM, Liou SJ (2004) J Appl Polym Sci 91:1368–1373
29. Noda N, Lee YH, Bur AJ, Prabhu VM, Snyder CR, Roth SC, McBrearty M (2005) Polymer 46:7201–7217
30. Jonscher AK (1983) Dielectric relaxation in solids. Chelsea Dielectric, London
31. Klein RJ, Zhang S, Dou S, Jones BH, Colby RH, Runt J (2006) J Chem Phys 124(144903):1–8
32. Fragiadakis D, Dou S, Colby RH, Runt J (2008) Macromolecules 41:5723–5728
33. Fragiadakis D, Dou S, Colby RH, Runt J (2009) J Chem Phys 130 (064907):1–11

34. Zhang S, Dou S, Colby RH, Runt J (2005) J Non-Cryst Solids 351:2825–2830
35. Dyre JC, Schrøder TB (2000) Rev Mod Phys 72:873–892
36. Dyre JC, Maass P, Roling B, Sidebottom DL (2009) Rep Prog Phys 72:046501–046515
37. Macdonald JR (2005) Phys Rev B 71:184307–184312
38. Kumar A, Deka M, Banerjee S (2010) Solid State Ion 181:609–615
39. Aranda P, Ruiz-Hitzky E (1999) Appl Clay Sci 15:119–135
40. Reinholdt MX, Kirkpatrick RJ, Pinnavaia TJ (2005) J Phys Chem B 109:16296–16303
41. Hikosaka MY, Pulcinelli SH, Santilli CV, Dahmouche K, Craievich AF (2006) J Non-Cryst Solids 352:3705–3710
42. Jaipal Reddy M, Kumar JS, Subba Rao UV, Chu PP (2006) Solid State Ion 117:253–256
43. Furlani M, Stappen C, Mellander BE, Niklasson GA (2010) J Non-Cryst Solids 356:710–714